International Journal of Engineering
Journal Homepage: www.ije.ir

Experimental Study of Polyvinyl Alcohol Nanocomposite Film Reinforced by Cellulose Nanofibers from Agave Cantala

F. Yudhanto[a,b], Jamasri*[a], H. S. B. Rochardjo[a], A. Kusumaatmaja[c]

[a] *Department of Mechanical and Industrial Engineering, Faculty of Engineering, Universitas Gadjah Mada, Indonesia*
[b] *Department of Mechanical Technology, Universitas Muhammadiyah Yogyakarta, Indonesia*
[c] *Department of Physics, Faculty of Mathematics and Natural Sciences, Universitas Gadjah Mada, Indonesia*

PAPER INFO

Paper history:
Received 20 October 2020
Received in revised form 16 December 2020
Accepted 14 January 2021

Keywords:
Polyvinyl Alcohol
Cellulose Nanofibers
Nanocomposite Film

ABSTRACT

This paper presents an experimental study of addition of cellulose nanofibers (CNF) extracted by the chemical-ultrasonication process from agave cantala leaf plants in the matrix of polyvinyl alcohol (PVA). Combining these materials produce the nanocomposite film with a thickness of 30 μm. The nanocomposite characteristic was investigated by the addition of CNF (0, 2, 5, 8, and 10 wt%) in PVA suspension (3 wt.%). PVA/CNF nanocomposite films were prepared by a casting solution method. The fibrillation of fibers to CNF was analyzed using Scanning Electron Microscopy and Transmission Electron Microscopy. The nanocomposite film functional group's molecular chemical bond and structural analysis were tested using Fourier Transform Infrared and X-ray diffraction. The PVA/CNF nanocomposite film has significant advantages on the ultraviolet barrier, thermal stability tested by Differential Scanning Calorimetry and Thermogravimetric Analyzer, and tensile strength. Overall, the optimal addition of CNF is 8 wt.% in matrix, resulting in the highest crystallinity index (37.5%), the tensile strength and elongation at break was an increase of 79% and 138%, respectively. It has good absorbing ultraviolet rays (82.4%) and high thermal stability (365ºC).

***doi**: 10.5829/ije.2021.34.04a.25*

1. INTRODUCTION

Cellulose is one of the main components of raw fibers and other constituent materials such as hemicellulose, lignin, and other extractive substances. The cellulose used in this study was obtained from agave cantala leaf plants that grew well in Sumenep regency, Madura, Indonesia. Cellulose was extracted and isolated through several mechanical, chemical, and combined processes to produce the cellulose nanofibers (CNF). The unique structure of the CNF has many advantages, like is biodegradable, biocompatible, large specific surface area, high modulus elasticity, low density, and a low coefficient of thermal expansion [1-4]. Some isolation methods that are often used to obtain CNF are mechanical processes, including the high-pressure homogenizer [5-6], grinding or disc refining [7], cyro-crushing [8], steam explosion [9], and high-speed blender [10].

This process requires a lot of energy and is less efficient in obtaining nanocellulose. Previous studies using isolation by chemical extraction and hydrolysis of strong acids were considered more efficient and did not require high costs and energy to produce nanocellulose. Purified fibers have been cleaned from impurities attached to fibers' surface, such as hemicellulose, lignin, pectin, and other contaminants. The purified fibers were obtained by using chemical extraction processes such as dewaxed, alkalization, and bleaching. The dewaxed process uses a solution of toluene and ethanol. At the same time, alkalization treated uses of potassium hydroxide (KOH), sodium hydroxide (NaOH), and the bleaching treated uses of sodium chlorite ($NaClO_2$), hydrogen peroxide (H_2O_2) solutions has been studied [9, 11-16].

*Corresponding Author Institutional Email: *jamasri@ugm.ac.id* (Jamasri)

Please cite this article as: F. Yudhanto, Jamasri, H. S. B. Rochardjo, A. Kusumaatmaja, Experimental Study of PVA Nanocomposite Film Reinforced by Cellulose Nanofibers from Agave Cantala, International Journal of Engineering, Transactions A: Basics Vol. 34, No. 04, (2021) 987-998

CNF isolation carried out using the hydrolysis process such as adding sulphuric acid (H_2SO_4), hydrochloric acid (HCl), nitrit acid (HNO_3) and acetic acid (CH_3COOH). It carried out after the process of purified fibers, and this process aims to open the microcellulose bundle into nanocellulose size. The previous studies have used a chemical extraction method, such as done by Listyanda et al. [17]. The ramie fiber has been isolated by adding sulphuric acid (H_2SO_4) solution of 41, 44, 47, 50 wt.% in the burette tube. The solution of sulphuric acid dropped slowly into the beaker and stirrer acid to pulp ratio (1:20) at the temperature of 45°C for 30 minutes to produce cellulose nanocrystal (CNC). Additional concentration of H_sSO_4 decrease the crystallinity index (CI) and thermal stability of CNC. The highest crystallinity index was obtained at 41 wt.%, leads from 79.7 to 90.7%. The average diameter and length are 6.26 nm and 106 nm, respectively (aspect ratio is 17).

The reported data by Kusmono and Akbar [18] have isolated the best fiber (ramie) using chemical extraction (alkali-bleaching) and hydrolyzed by hydrochloric acid (HCl). At various concentrations of 6, 8, and 12 M of HCl at the temperature of 45°C for the different times of hydrolysis were 70, 125, 180 minutes. Additional concentration of HCl does not influence the crystallinity index and thermal stability. The long hydrolysis time was decreased the crystallinity index (CI) and thermal stability. The optimum condition process to produce CNC at a concentration of 6 M of HCl at the temperature of 45°C for 70 minutes. It creates a rod-like shape of CNC with a high CI from 79.75 to 89.61%, crystallite size 5.81 nm, and the average diameter and length are 8 nm, 158 nm, respectively (aspect ratio is 20).

Krishnadev et al. [19] have isolated the leaf fiber (*Agave Americana*) with chemical extraction (alkali, bleaching) and acid hydrolysis (nitrite acid combined with acetic acid) at temperature 100°C for 30 minutes. This chemical process, coupled with ultrasonication, produces cellulose nanofibers with average diameters 18.2 ± 10 nm, confirmed by TEM. The CNF has a crystallinity index of 64.1% higher than raw fiber is 50.1%.

Zakuwan and Ahmad [20] have isolated kenaf fiber using 65 wt.% sulphuric acids at a preheat temperature of 45°C for 40 minutes to produces CNC with average diameter and length of 12-15 nm and 101-260 nm, respectively and result in an aspect ratio of 8-17. The high aspect ratio and crystallinity index were significant in improving the reinforcement of nanocomposites. [21-23].

Nanocellulose is known to their high moisture absorption, which leads to a decrease in mechanical properties. To overcome this problem, adding other hydrophilic biocompatible polymers is necessary to remove the reactivity of hydroxyl groups of the nanocellulose. The polymer used as a matrix in the manufacture of nanocomposite films is polyvinyl alcohol (PVA). PVA is easily dissolved in water and biodegradable polymers, resistance to chemical conditions, so it is an attractive material used as an application based on advanced technology. PVA is also non-toxic on the human body and can be used to manufacture medicine cachets, drug delivery systems, barrier materials, membranes, and yarn for surgery [24-25]. The use of PVA for environmentally friendly food packaging began widely used due to several advantages of PVA, including strength, transparent, lightweight, non-toxic, heat-stable, antimicrobial, and good elasticity [26-28].

There are several parameters characteristics of CNF reinforced PVA nanocomposites such as diameter (D), length (L), aspect ratio (L/D), volume fraction ($\%V_f$), adhesion bond between nanocellulose and matrix, and dispersion the nanocellulose in the matrix [29].

This research's main objective is to produce nanocomposite film, which has high mechanical strength, stiffness, and ultraviolet absorbance by adding gel CNF. The made of CNF by the extraction-ultrasonication process. The mix of CNF and matrix PVA to be homogeneous is an essential factor to obtained the homogeneous solution. Physical properties, UV absorbance, and thermal stability were evaluated by XRD, FTIR, SEM, TEM, UV-Vis (Ultraviolet and Visible) transmittance, as well as DSC and TGA tests. The mechanical properties were tested by tensile strength with UTM (Universal Testing Machine).

2. MATERIALS AND METHODS

2.1. Materials The PVA $(C_2H_4O)x$ (fully hydrolyzed, the density of 1.19 g/cm^3 and molecular weight of 145000 Da) was supplied from Sigma Aldrich. Nanocellulose used was isolated from the Agave Cantala was obtained from Sumenep, Madura island, Indonesia. The chemical solution for the process of dewaxed, alkalization, bleaching, and hydrolysis. The solution used there are toluene, ethanol, sodium hydroxide (NaOH), hydrogen peroxide (H_2O_2) and sulphuric acid (H_2SO_4) were supplied by CV. Wahana Hilab Indonesia, Yogyakarta.

2. 2. Isolation of Cellulose Nanofibers (CNF) Cantala fiber, obtained from the leaf, it was cut into small pieces with a size of approximately 10 mm. Chemical pretreatment in cantala fibers includes dewaxing using a soxhlet contain toluene and ethanol solution (2:1) vol.% for 6 hours (20 cycles) [11], [30]. The alkalization process used 5 wt.% NaOH solution at 100°C for an hour, followed by bleaching using 3 wt.% H_2O_2 at pH 10 at a temperature of 60°C for an hour.

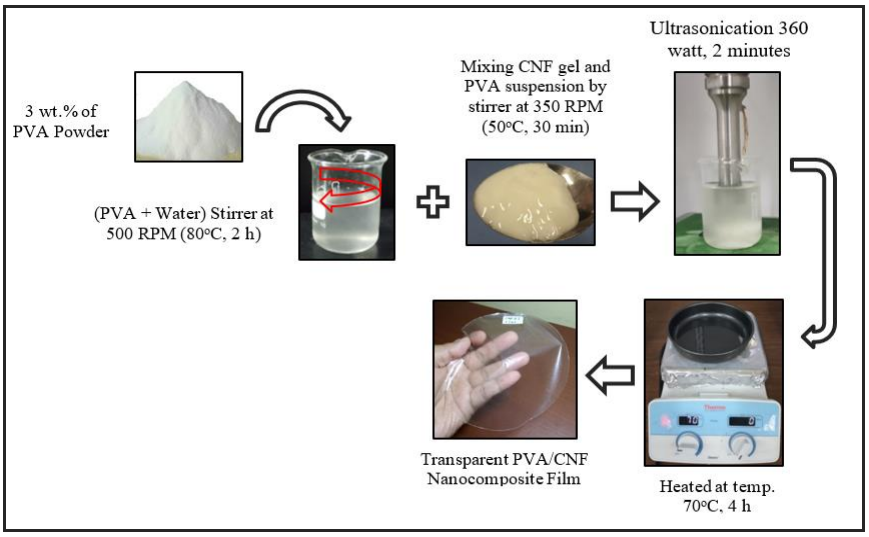

Figure 1. Schemes to produce of PVA/CNF nanocomposites film

The purified fibers were put in an Erlenmeyer flask and placed on a magnetic stirrer with a rotating of 350 RPM [31]. The hydrolysis process used concentration 44 wt.% of the H_2SO_4 solution. It was dripped slowly into an bekker glass from a burette tube. The suspension of CNF was adjusted to constantly rotate slowly with magnetic stirrer (200 RPM) at the pre-heat temperature 60°C for an hour. The suspension of CNF put into the cooled water bath at the temperature of 5°C for 30 minutes to stop acid hydrolysis reaction. Both the suspension was rinsed in the deionized water by centrifuged at 4 cycles and neutralized with NaOH until pH 7.

Fiber fibrillation in the suspension was assisted by an ultrasonic homogenizer (600 watt max. output), which aims to obtain uniform scale of nano sizes. This process was carried out at 20-25 kHz sound waves, 40 % output power (240 watt) using a 6 mm diameter probe for an hour at temperatures of 60°C, and produce a cellulose nanofibers suspension

2. 3. Preparation of PVA/CNF Nanocomposite The CNF liquid suspension was centrifuged at 4000 RPM for 10 minutes to obtain CNF gel. The PVA suspension was prepared by adding the 3 wt.% of PVA powder into pure water at temperature 80°C and stirring at 500 RPM for 2 hours. The PVA suspension was subsequently put into a desiccator containing silica gel for one night to remove the bubbles in the suspension. The CNF gel was prepared with a concentration of 0, 2, 5, 8 and 10 wt.%. The CNF gel and PVA suspension were constantly mixed with stirrer at 350 RPM at temperature 50°C for 30 minutes and followed by ultrasonication with 60% output power (360 watt) for 2 minutes to obtain homogeneous solution [32]. The homogenization process is very important to homogen dispersed CNF in the PVA. The PVA/CNF suspension then casting into a teflon plate, which has dimension is 150 mm in diameter and heated for 4 hours at 70°C (Figure 1).

2.4. Morphology of Fibers Morphology of the fiber was observed by SEM (JSM-6510, LA type JEOL) and TEM (JEM 1400 type, JEOL) characterization to obtain the diameter size (D), and fiber length (L). The Measurement of aspect ratio (L/D) uses imaging analysis program Image J with 20 sample of single nanocellulose. Operating SEM voltage was set 40 kV condition. Test specimen coated with Au and using sputtering technique. Operating TEM voltage was set range from 40 to 120 kV, to get very high contrast and was capable of magnification from 200 to 1,200,000 times.

2. 5. XRD Characterization The XRD patterns of raw fiber and nanocomposite films were measured by using the Rigaku Miniflex-600 type. It was running at 40 kW operating power conditions, and 15 mA current using Cu Kα radiation with wavelength 1.540 Å. Powder sample of XRD test scanned in 2θ range varying from 3° to 40° with an average scan rate of data 2° min^{-1}. The CI (Crystallinity Index) of the organics material is determined by the Segal, as follows in Equation (1) [33]:

$$\mathbf{CI} = \frac{I_{002} - I_{amor}}{I_{002}} \quad \textbf{(1)}$$

I002 is the intensity of the 002 peaks, which represents the crystalline structure approximately at 2θ = 22°, Iamor is the lowest peak intensity at 2θ=18° represents the amorphous structure.

2. 6. FTIR Characterization FTIR spectra was used to determine the functional bonding groups of materials through changes in the intensity of electromagnetic waves. Wavelengths were measured from a range of 400 to 4000 cm^{-1}. The Shimadzu 8400S spectrometer was used to characterize the materials prepared by blending with potassium bromide (KBr) and followed by pressing to obtain a thin film.

2. 7. Transmittance UV-Vis The ultraviolet (UV) absorption and Visibilty (Vis) of material transparency were characterized by the Ocean Optics USB 4000 spectrophotometer. This characterization was aimed to determine the UV absorption value and its visibility.

2. 8. Mechanical Properties Characterization Tensile strength and elongation at break in the nanocomposite film material were measured by Universal Testing Machine (Pearson Panke Equipment Ltd) with a maximum tensile strength of 200 N and the cross-head speed set of 2 mm/min. The dimension of the tensile test specimen of the plastic film utilized ASTM D-882, for the plastic film thickness from 0.025 to 1 mm, the width and gauge length were 5 mm and 250 mm, respectively.

2. 9. TGA Characterization The thermal stability was performed by a TGA (thermal gravimetry analyzer) and DTG (Diferential Thermal Gravimetry) test was used to calculate the weight of degradation. The TGA characterization is set up in range of 3 to 700 ^oC, with a temperature rate of 10 ^oC min^{-1} using 50 ml/min nitrogen gas (N_2). The test equipment used is the TGA Mettler Toledo model.

2. 10. DSC Characterization DSC (Differential Scanning Calorimetry) was used to determine thermal parameters and the degree of crystallinity mechanism of materials in a polymer system [34]. The tools used are the DSC-60 Plus and Flow Unit Control, and also use the TA-60WS Collection Monitor software on the desktop. The sample is heated at 30-250 °C with Nitrogen Gas, where the flow rate is 10 ml/min. The degree of crystallinity index could be calculated by estimating enthalpy fusion of endotherms curve of DSC. The degree of CI for polymer as follow the Equation (2) [35],

$$X_c = \frac{\Delta H_f(T_m)}{\Delta H_f{}^o(T_m{}^o)} \quad (2)$$

where Xc is the weight fraction degree of crystallinity, $\Delta H_f\ (T_m)$ is the enthalpy of fusion measured at the melting point T_m and $\Delta H_f^o\ (T_m{}^o)$ is enthalpy of fusion of totally crystalline the PVA polymer measured at equilibrium melting point $(T_m{}^o)$ is a 138.6 jg^{-1} [36]. The crystallinity index could be calculated using Equation (3) [35].

$$X_c = \frac{\Delta H_f(T_m)}{\Delta H_f{}^o(T_m{}^o)(1-m_f)} \quad (3)$$

where m_f is the mass fraction filler of CNF in nanocomposite film. The important properties of the polymer system are ussualy related to the structural of crystallinity index (CI).

3. RESULTS AND DISCUSSION

3. 1. Morphology of Cellulose Fibers Figure 2 shows the SEM (Scanning Electron Microscope) image of the cantala fiber before and after the chemical extraction (dewaxed-alkali-bleaching-sulphuric acid hydrolysis 44 wt.%). The bundle raw fibers were composed of individual cellulose linked together by massive cementing material like hemicellulose, lignin and pectin (Figure 2a). It has a diameter between 120-180 μm, the chemical composition of raw agave cantala fiber is cellulose 48.97%, hemicellulose 34.41 %, lignin 11.76 % and other substance 4.86 % [31].

Figure 2b shows the image of treated fiber after dewaxed-alkali process. The most of hemicellulose was damaged and removal became alkali-soluble, but some part of the lignin is still attached to the surface of fibers. The bleaching process aim to remove the lignin structure. The bleaching process with hydrogen peroxide strongly influence the removal most lignin on the surfaces of fibers and also accompanied partially fibrillated the bundle cellulose. The diameter of the cantala fiber after the bleaching process decrease from 30 μm to 60 μm. The surfaces of fiber after the chemical extraction look like clean and more roughness (Figure 2c). In Figure 2d, it is also shown that the diameter of the fiber dramatically changes after the hydrolysis. It causes decreased the diameter of the fiber ranges from 5 ± 2 μm.

Hydrolysis using sulfate acid (H_2SO_4) aims to open a cellulose bundle with a long cellulose chain that will break up into short individual cellulose. The diameter of cellulose bundles also changes from micro to nano size. Sulfate ions have separated the amorphous region (hemicellulose and lignin), and the crystalline region became the individual cellulose nanofibrils, as shown in Figure 3.

The chemical extraction process in fibers produces CPF (chemical purified fiber). It increased the cellulose by 71.58 % and decreased the hemicellulose by 18.45 % and lignin by 6.13 % [31]. The hydrolysis had a significant effect on reduced the lignin structure in the fiber.

The hydrolysis process starts from the breaking of oxygen bonds in the β-1,4-Glycosidic chain, then proceed with the separation of the glycosidic ring bonds and reacts with water (H_2O) were resulted from the

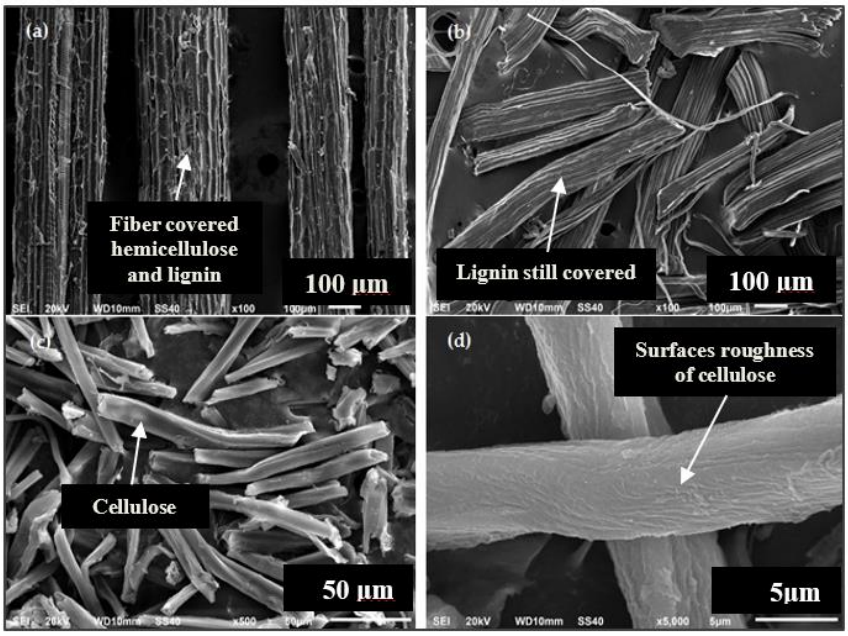

Figure 2. SEM image of (a) raw fiber, (b) treated fiber after alkali, (c) treated fiber after bleaching (d) individual cellulose after sulphuric acid hydrolysis

hydrolysis process of strong acids. Finally, the opening phase of the cellulose rings. Sulfate Acid is a strong acid, in water (H_2O) fully ionized to form hydronium ions (H_3O^+) and hydrogen sulfate (HSO_4^{2-}) (Figure 4).

Ultrasonication process after the hydrolysis process results in an individual CNF which bond together forming the web-like structure could be shown in the TEM image (Figure 5). The web-like structure shaped of cellulose nanofibers (CNF) were calculated by image-J of their length (L), diameter (D) to obtain the aspect ratio (L/D). It is well known that the aspect ratio of CNF affected the crucial role in their reinforcing capabilities [15,31]. The average diameter and length of CNF agave cantala are 45 nm and 1975 nm, respectively; resulting the aspect ratio is 43,8 (Figure 5), it show the high aspect ratio of CNF.

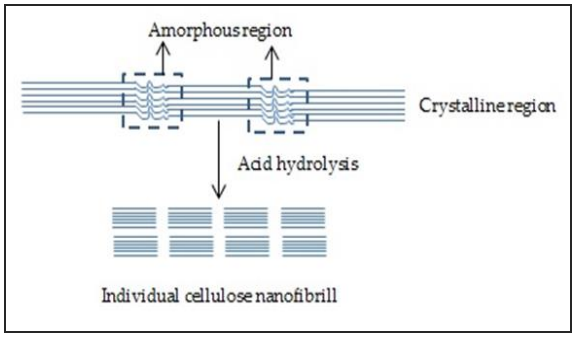

Figure 3. Schematic illustration disintegrated of amorphous region and crystalline region

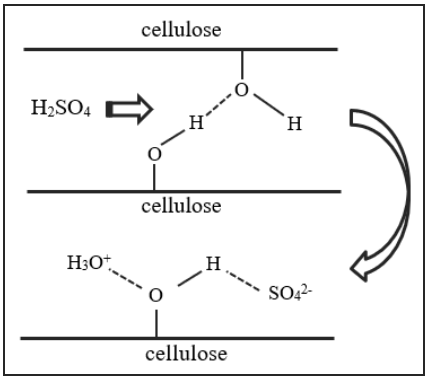

Figure 4. Schematic illustration of chemical reaction of bundle cellulose to individual cellulose by sulphuric acid hydrolysis

The previous study by Siqueira et al. [42], a similar *Agavaceae* family species, the aspect ratio of CNF agave sisalana fibers is 43. The aspect ratio from another fibers that were extracted from agronomy plant source such as coconut husk by 5.5 ± 1.5 nm [37], rice straw by 17 nm, poplar wood by 43 nm, white straw by 45.2 nm [38], soy hulls by 4.43 ± 1.20 nm [39], rice straw by 17 nm [40] and sugarcane bagasse by 4 ± 2 nm [41].

3. 2. Morphology of Nanocomposite Film

Figure 6 is SEM image shows the neat PVA nanocomposite films without the CNF. The neat PVA nanocomposite films show the transparent film, and the

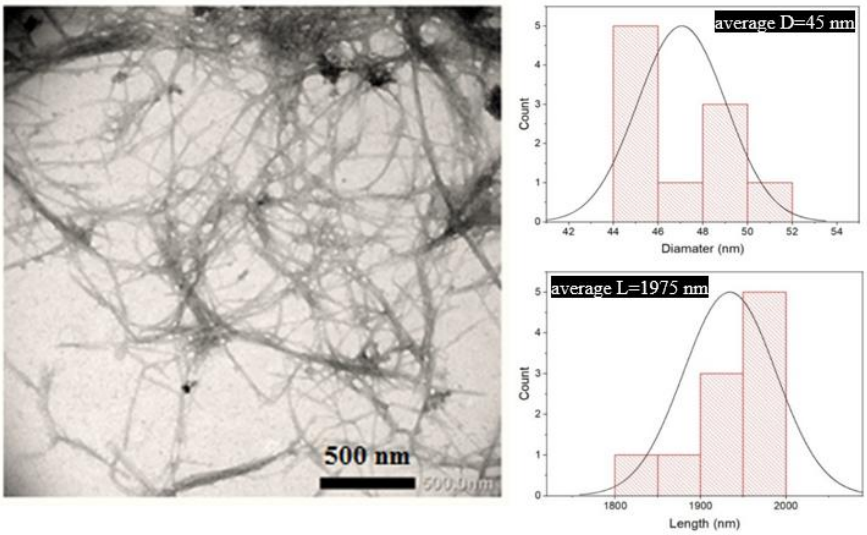

Figure 5. TEM image of diameter and length distribution of cellulose nanofibers (CNF)

polymers distributed uniformly. Figure 7 shows of the 8 wt.% of CNF in the PVA matrix, and it appears that CNF (web like structure) could be well distributed. The good dispersion of the CNF is the major factor to determine the mechanical properties of the nanocomposite film.

However, we founded the agglomerate CNF in the small areas in PVA nanocomposite film. Addition of 10 wt.% CNF causes the aglomeration evenly distributed in some areas on PVA matrix lead to 10-12% (Figure 8). The concentration of 10wt.%. of CNF causes the occurrence of piles of nanocellulose which formed the agglomeration.

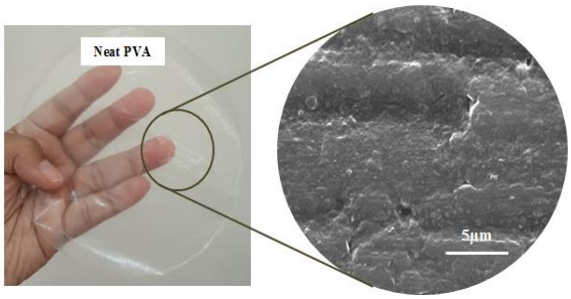

Figure 6. Photo SEM of Neat PVA nanocomposite film

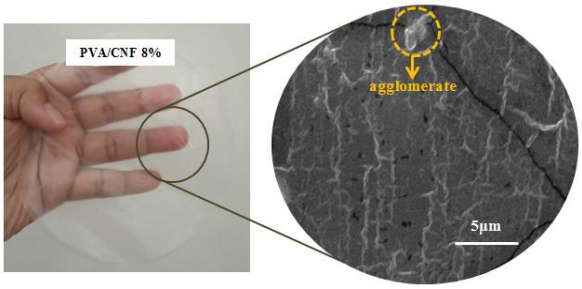

Figure 7. Photo SEM of PVA/CNF 8% nanocomposite film

3. 3. XRD Characterization Nanocomposite Film

Figure 9 (a) shows the X-ray diffractogram graph of raw fiber and CNF. The major intensity patterns in the CI of the raw fiber and CNF are peaks at $2\theta = 16.49^{o}$, 22.84^{o} and 34.88^{o}, from the JCPDS (Joint Committee on Powder Diffraction Standards) card of native cellulose (PDF # 030289) shows the crystalline plane is 111, 002, and 040, respectively; indicates the cellulose type I [31, 43, 50]. The amorphous region at the peak a $2\theta = 18^{o}$. The highest intensity peaks at a $2\theta = 22.84^{o}$ show a significant increase of cellulose, indicating the amorphous material such as hemicellulose and lignin removal. The correlation changes of the crystalline plane structure from alpha-cellulose (Iα) to beta cellulose (Iβ) due to the chemical-ultrasonication process increase the CI from 64.5% to 78.2%. The beta

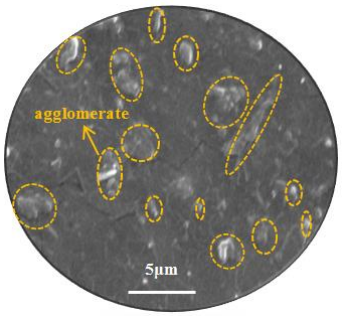

Figure 8. Photo SEM of PVA/CNF 10% nanocomposite film

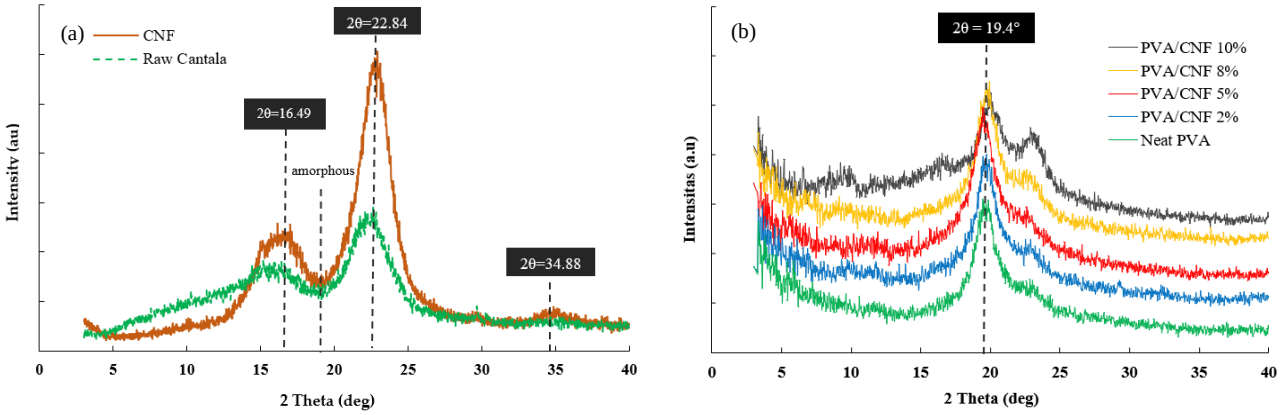

Figure 9. The XRD patterns of (a) raw fiber and CNF, (b) various nanocomposite film

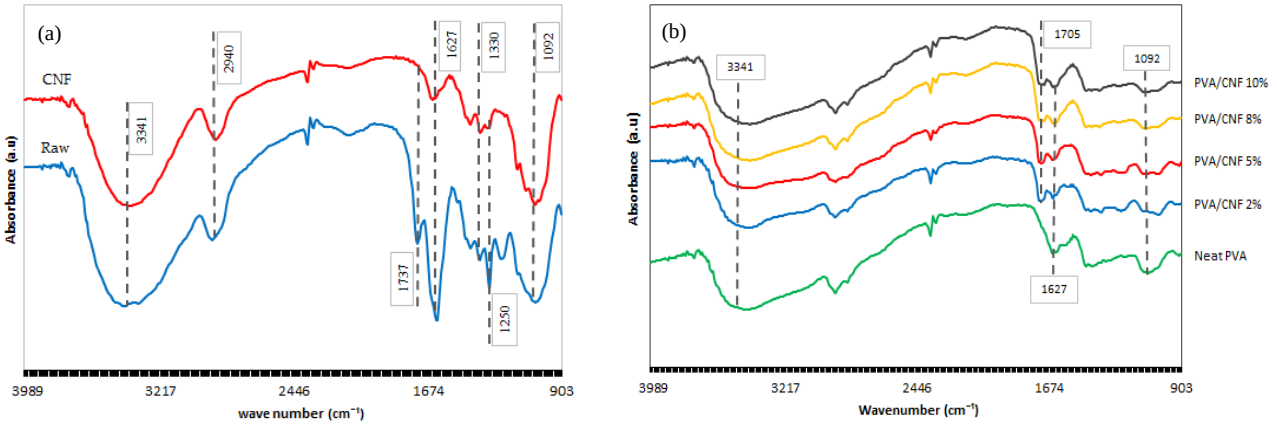

Figure 10. The FTIR patterns of (a) raw fiber and CNF, (b) various nanocomposite film

cellulose (Iβ) has two cellulose hydrogen bonds and is more stable, stronger than alpha cellulose which has only one cellulose hydrogen bond [32, 41].

The X-ray diffractions nanocomposite films showed in Figure 9 (b). The crystallinity index of neat PVA film at 2θ=19.4 is 30.7% compared to the other nanocomposite film. The addition CNF of 2, 5, and 8 wt.% had increased the CI values to 32.0%, 35.8%, and 37.5%, respectively. The relation between increasing the CI values and stiffness of cellulose, where the high CI could be raised the stiffness of cellulose [43]. The higher mechanical strength of nanocomposite film correlated with a higher crystallinity index of CNF. More than 8% CNF in the matrix caused a decrease of CI by 22.9% and impacted mechanical properties decreased.

3. 4. FTIR Characterization of Nanocomposite Film Figure 10 (a) shows the FTIR spectroscopy to determine the physical structure and functional groups of the lignocellulosic plant. The absorbance peak of a raw fiber at 1250 cm^{-1} corresponds to C-O stretching in the acetyl group. The C=O stretching on carbonyl in ester bonds is shown at wavenumber 1737 cm^{-1} [38, 43-44] there are indicating the presence of hemicellulose and lignin.

Many functional groups of acetyl and uronic ester groups forming hemicellulose and carboxylic groups of ferulic lignin-forming [38]. The peak wavelength of 1627 cm^{-1} indicates the absorbance of water [12-13], [15].

The absorption 1092 cm^{-1} the asymetry ring pyranose C-O-C showed that existance the content of an hydroglucose in the cellulose I [45]. The absorption at 1330 cm^{-1} is attributed to CH_2 symmetric bending and C-O aromatic ring polysaccharides. The peak of 2924 cm^{-1} shows aliphatic saturated C-H stretching vibration in cellulose [15]. The wavenumber 3340-3342 cm^{-1} shows the intramolecular hydrogen bonding (-OH) group of cellulose [45].

Figure 10 (b) shows the FTIR spectra graph of PVA nanocomposite films' peak in various addition of CNF.

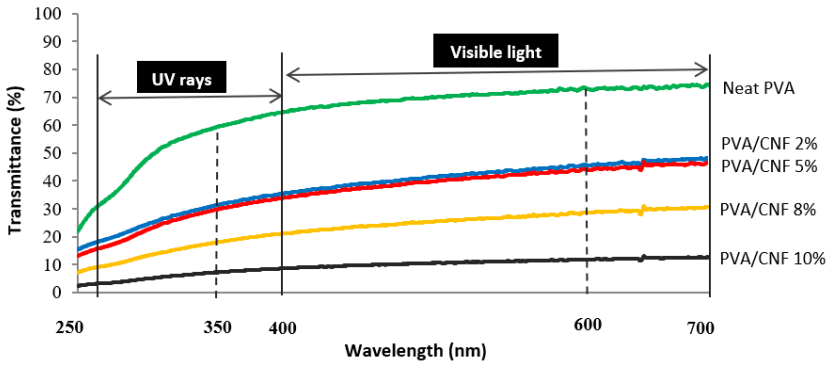

Figure 11. The UV-Vis spectra anaysis of nanocomposite film

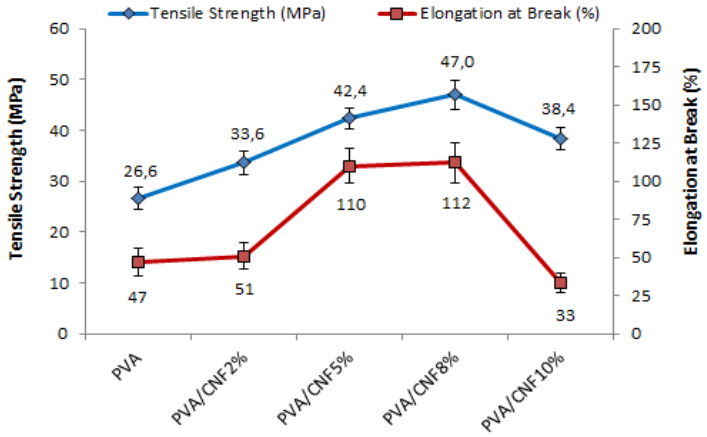

Figure 12. The Tensile strength and elongation at break of nanocomposite film

The sharp peaks waveform change into ramps at the range of 1092 cm^{-1} (C-O-C stretching) and 3341 cm^{-1} shows that monosaccharides that cellulose bond-forming begin to strongly cross-linked with the matrix. In the previous research conducted by Lim et al. [46], PAA hydrogel material and cellulose nanocrystals showed a good bond even though the two materials retain their unique characteristics which changes–the intensity and shape of peaks at waveform 1054-1092 cm^{-1}. Addition of CNF also reduces the water absorbance, which may cause the adhesion bonding between hydrophilic properties in PVA with CNF material, as shown waveform pattern at 1627cm^{-1}.

3. 5. The UV-Vis Absorbance of Nanocomposite Film Figure 11 shows that the CNF addition is also affecting the transparency of the film, which seems to decrease slightly. The visible light spectroscopy, it is shown that the neat PVA nanocomposite film has an excellent visible light transmittance is 73%. Addition of 2, 5, 8, and 10 wt.% of the CNF in the matrix had decreased the visible light transmittance to 45, 43.3, 28 and 11.7%, respectively, but raises the absorbance of The UV rays at 350 nm wavelength.

The percentage absorb of UV rays in the PVA nanocomposite is a little (41.8%). Addition of 2, 5, 8, and 10 wt.% of CNF causes an increase in the absorb UV rays significantly became 69.2, 70.8, 82.4, 92.9 %. The small transmittance is indicating the material has strong absorbance of UV rays. The cellulose and lignin in the CNF significantly influence the absorption of UV rays and visible light. The lignin has a complex structure polydispersity in molecular weight to absorb the UV [47]. The excellent UV absorbance and still good transparency are PVA/CNF 8% (UV absorbance is 82.4%, and visible transmittance light is 28%).

3. 6. Mechanical Properties Figure 12 indicates the effect of CNF on tensile strength and elongation at the break of the nanocomposite films. From the mechanical test, addition of CNF to the PVA matrix would increase the nanocomposite's mechanical properties. Generally, an increase in CNF would increase the tensile strength and elongation at break.

The neat PVA has 26.6 MPa in tensile strength and 47% in elongation at break. Addition of 2 wt.% CNF did not give significant effect at mechanical properties because the CNF undispersed in the PVA matrix. Whereas the addition of 8 wt.% of CNF gives a substantial improvement in the mechanical properties, It increase the tensile strength and elongation at break are 79% and 138%, respectively. This condition shows that CNF has distributed well in the matrix, and it causing the homogeneous stress of nanocomposite film. The homogeneous stress leads that the excellent polymer branching bonds between the hydroxyl group (-OH) in the nanocellulose and carbonyl groups (C=O) in the matrix's polymer chain.

3. 7. DSC Thermal Analysis DSC (Differential Scanning Calorimetry) is one of the necessary tests to determine the thermal parameter such as a glass transtition (T_g), phase changes, melting purity crystallization (T_m), heat capacity (ΔH_m) and degree of crystallinity (X_c) of the polymer. According to Agrawal et al. [48] the PVA is one of the partially crystalline polymers exhibiting both the glass transition temperature, T_g (characteristic of amorphous phase) and melting iso-therm, T_m (characteristic of crystalline phase).

Figure 13 and Table 1 show the glass transition and melting temperature on Neat PVA and PVA/CNF nanocomposite films. The neat PVA films show glass transition temperature at 85ºC. The addition of CNF 2, 5 and 8 wt.% increases the glass transition and the melting temperature. Addition of CNF 10 wt.% causes the decrease the glass transition and melting temperature. It's causes chemical bonding starting weakness and then the hydroxyl group in cellulose easily absorbs the heat.

This resutl is slighty different with the previous research by Patel et al. [35], addition of 5, 10, 15, and 20 wt.% of palm leaf (PL) nanocrystalline powder in PVA films has increased melting temperature (T_m), but it did not happen on a glass transition temperature (T_g). That addition does not significant change T_g material of PL/PVA.

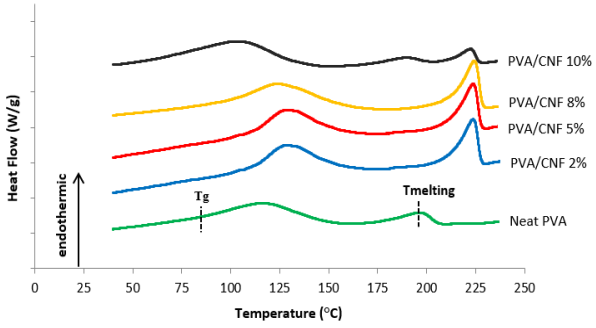

Figure 13. The DSC melting result of nanocomposite film

TABLE 1. The transition glass and melting temperature nanocomposite film

Samples	T_g (in ºC)	T_m (in ºC)	ΔH_m (in J/g)	X_c (in %)
Neat PVA	85	195	30.8	22.2
PVA/CNF 2%	106	230	48.6	35.8
PVA/CNF 5%	108	225	47.3	35.9
PVA/CNF 8%	102	225	55.5	43.5
PVA/CNF 10%	65	189	20.2	16.2

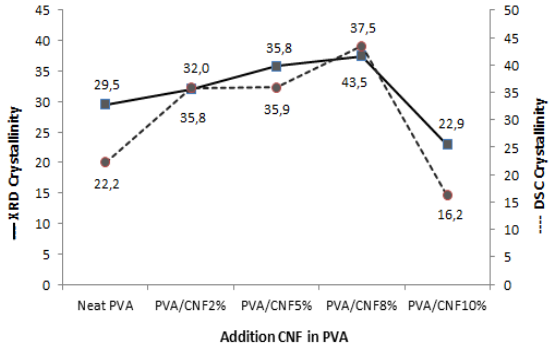

Figure 14. The crystallinity index from XRD and DSC test

Figure 14 shows the enthalpy fusion of DSC could determine the degree of crystallinity index (CI). The CI pattern from DSC results has a similar correlation with XRD spectra result. Addition of CNF from 2 to 8 wt.% had increased the CI of nanocomposite film and after more than 8 wt.%, the CI decreased. It's indicated the some crystalline region starting degraded in the molecular bond at initial temperature.

3. 8. Thermogravimetric Analysis Figures 15 and 16 show the thermogravimetric Analysis (TGA) and derivative thermogravimetric (DTG) of nanocomposite film. The weight loss and derivative weight of nanocomposite films that occur by changing the temperature, which indicated by T_{onset} (the initial degradation of material), $T_{10\%}$ (the weight loss of 10% material), and T_{max} (the maximum of degradation). In this study the T_{onset} to T_{max} of neat PVA film occur at temperature from 213 ºC to 275 ºC (MW = 145,000 Da), slightly higher than the the previous study by Rynkowska et al. [49] at temperature from 210 ºC to 265 ºC (MW = 100,000 Da), its due to the differences in molecular weight (MW).

Typically, initial decomposition of the lignocellulosic material has been started above at 200ºC, it occurs due to the evaporation of adsorbed moisture and the remaining hemicellulose's burning earlier. In all cases, the initial weight loss quickly occurs in the remaining isolation results in the hemicellulose contain the acetyl functional groups. The decomposition of the

hemicellulose region firstly occurs before lignin and cellulose [37]. Addition of CNF as reinforcement in PVA can increases the thermal stability of nanocomposite films. This behavior caused the CNF has a well alignment crystallite structure so that the nanocomposite film has high stability thermal at the temperature above at 300ºC.

Table 2 shows the increase of thermal stability in each variation of nanocomposite film. Addition of CNF 2 to 5 wt.% could increase maximum thermal degradation (T_{max}) to 310ºC, 340ºC and 365ºC, respectively. Addition of 10 wt.% CNF causes the slightly decreases the thermal stability to 363ºC. It's

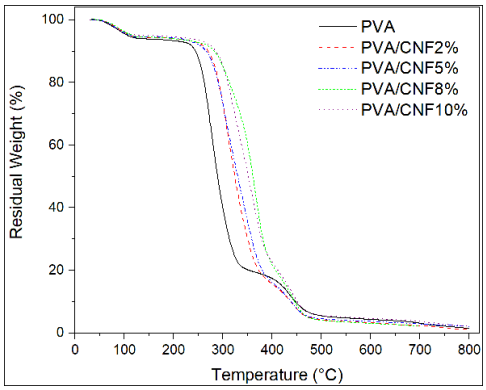

Figure 15. The graph of Thermal Gravimetri Analyze (TGA)

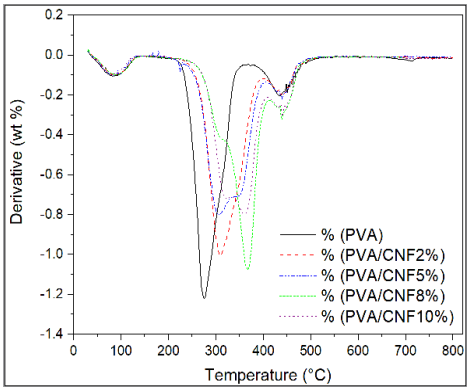

Figure 16. The graph of Differential Thermal Gravimetry (DTG)

TABLE 2. TGA Result of Neat PVA and PVA/CNF nanocomposite film

Samples	T_{onset} (in ºC)	T_{max} (in ºC)	$T_{10\%}$ (in ºC)
PVA	213	275	244
PVA/CNF 2%	225	310	270
PVA/CNF 5%	215	340	265
PVA/CNF 8%	251	365	282
PVA/CNF 10%	250	363	285

caused the crystallite structure linkages between cellulose and the matrix beginning unstable.

4. CONCLUSION

The effect of 8 wt.% CNF on the PVA film matrix can improve the physical properties and mechanical strength. The FTIR and XRD test shows that a good dispersion and high mechanical interlocking between CNF and PVA. The crystallinity index was increased from 29.5% to 37.5%. The tensile strength and elongation at break were increased from 26.6 to 47 MPa and 47% to 112%, respectively. The high thermal stability indicates the shift lead the glass transition temperature (T_g) from 85ºC to 102ºC and the maximum degradation temperature (T_{max}) from 275ºC to 365ºC. Based on the characterization results, it's shown that nanocomposite film has the highest mechanical strength, UV barrier, transparent, and high thermal stability.

5. ACKNOWLEDGEMENT

This research was carried out under a dissertation grant by Ministry of Finance of The Republic Indonesia through Lembaga Pengelola Dana Pendidikan (LPDP) BUDI-DN scholarship program No. PRJ-1427/LPDP.4/2019.

6. REFERENCES

1. Kumar, Ritesh, Sanju Kumari, Shivani Singh Surah, Bhuvneshwar Rai, Rakesh Kumar, Sidhharth Sirohi, and Gulshan Kumar. "A simple approach for the isolation of cellulose nanofibers from banana fibers." ***Materials Research Express,*** Vol. 6, No. 10, (2019), 105601. doi: 10.1088/2053-1591/ab3511
2. Syafri, Edi, Anwar Kasim, Hairul Abral, and Alfi Asben. "Cellulose nanofibers isolation and characterization from ramie using a chemical-ultrasonic treatment." ***Journal of Natural Fibers,*** (2018). doi: 10.1080/15440478.2018.1455073
3. Meng, Fanrong, Guoqing Wang, Xueyu Du, Zhifen Wang, Shuying Xu, and Yucang Zhang. "Extraction and characterization of cellulose nanofibers and nanocrystals from liquefied banana pseudo-stem residue." ***Composites Part B: Engineering,*** Vol. 160, (2019), 341-347. doi: 10.1016/j.compositesb.2018.08.048
4. Moon, Robert J., Ashlie Martini, John Nairn, John Simonsen, and Jeff Youngblood, "Cellulose nanomaterials review: structure, properties and nanocomposites." ***Chemical Society Reviews***, Vol. 40, (2011), 3941-3994. doi: 10.1039/c0cs00108b
5. Panyasiri, Panee, Naiyasit Yingkamhaeng, Nga Tien Lam, and Prakit Sukyai. "Extraction of cellulose nanofibrils from amylase-treated cassava bagasse using high-pressure homogenization." ***Cellulose,*** Vol. 25, No. 3, (2018), 1757-1768. doi: 10.1007/s10570-018-1686-6
6. Ilyas, R. A., S. M. Sapuan, M. R. Ishak, and E. S. Zainudin. "Sugar palm nanofibrillated cellulose (Arenga pinnata (Wurmb.)

Merr): effect of cycles on their yield, physic-chemical, morphological and thermal behavior." ***International Journal of Biological Macromolecules***, Vol. 123 (2019), 379-388. doi: 10.1016/j.ijbiomac.2018.11.124

7. Supian, Muhammad Arif Fahmi, Khairatun Najwa Mohd Amin, Saidatul Shima Jamari, and Shahril Mohamad. "Production of cellulose nanofiber (CNF) from empty fruit bunch (EFB) via mechanical method." ***Journal of Environmental Chemical Engineering,*** Vol. 8, No. 1, (2020), 103024. doi: 10.1016/j.jece.2019.103024
8. Bhatnagar, A., and M. Sain. "Processing of cellulose nanofiber-reinforced composites." ***Journal of Reinforced Plastics and Composites,*** Vol. 24, No. 12, (2005), 1259-1268. doi: 10.1177/0731684405049864
9. Song, Yan, Wei Jiang, Yuanming Zhang, Haoxi Ben, Guangting Han, and Arthur J. Ragauskas. "Isolation and characterization of cellulosic fibers from kenaf bast using steam explosion and Fenton oxidation treatment." ***Cellulose,*** Vol. 25, No. 9, (2018), 4979-4992, doi: 10.1186/s40201-015-0167-1
10. Rochardjo, H.S.B Jamasri and Yudhanto, F. "Extraction of Natural Fibers by High-Speed Blender to Produce Cellulose Sheet Composite." ***International Review of Mechanical Engineering,*** Vol. 13, No. 12, (2019), 691-699. doi: 10.15866/ireme.v13i12.17586
11. Abe, Kentaro, and Hiroyuki YaNo. "Comparison of the characteristics of cellulose microfibril aggregates of wood, rice straw and potato tuber." ***Cellulose,*** Vol. 16, No. 6, (2009), 1017-1023. doi: 10.1007/s10570-009-9334-9.
12. Yudhanto, F. and Rochardjo, H.S., "Application of taguchi method for selection parameter bleaching treatments against mechanical and physical properties of agave cantala fiber." In ***IOP Conference Series: Materials Science and Engineering***, IOP Publishing, Vol. 352, (2018), 012002. doi:10.1088/1757-899X/352/1/012002
13. Yudha, V., Rochardjo, H.S.B., Jamasri, J., Widyorini, R., Yudhanto, F. and Darmanto, S., "Isolation of cellulose from salacca midrib fibers by chemical treatments." In ***IOP Conference Series: Materials Science and Engineering***, IOP Publishing, Vol. 434, (2018**)**, 012078. doi: 10.1088/1757-899X/434/1/012078
14. Carvalho, Kelly Cristina Coelho, Daniella Regina Mulinari, Herman Jacobus Cornellis Voorwald, and Maria Odila Hilário Cioffi, "Chemical modification effect on the mechanical properties of hips/coconut fiber composites." ***BioResources***, Vol. 5, (2010**)**, 1143-1155. doi: 10.4186/ej.2012.16.2.73
15. Kargarzadeh, Hanieh, Ishak Ahmad, Ibrahim Abdullah, Alain Dufresne, Siti Yasmine Zainudin, and Rasha M. Sheltami, "Effects of hydrolysis conditions on the morphology, crystallinity, and thermal stability of cellulose nanoc extracted from kenaf bast fibers." ***Cellulose***, Vol. 19, (2012), 855-866. doi: 10.1007/s10570-012-9684-6
16. Rizal, Samsul, Deepu Gopakumar, Sulaiman Thalib, Syifaul Huzni, and H. Abdul Khalil, "Interfacial compatibility evaluation on the fiber treatment in the typha fiber reinforced epoxy composites and their effect on the chemical and mechanical properties." ***Polymers,*** Vol. 10, (2018), 1316. doi: 10.3390/polym10121316.
17. Listyanda, R. Faiz, Kusmono, Muhammad Waziz Wildan, and Mochammad Noer Ilman. "Extraction and characterization of nanocrystalline cellulose (NCC) from ramie fiber by sulphuric acid hydrolysis." In ***AIP Conference Proceedings***, Vol. 2217, No. 1, p. 030069. AIP Publishing LLC, (2020). doi: 10.1063/5.0001068.
18. Kusmono, K. and Akbar, D.A., "Influence of Hydrolysis Conditions on Characteristics of Nanocrystalline Cellulose Extracted from Ramie Fibers by Hydrochloric Acid Hydrolysis." (2020), doi: 10.21203/rs.3.rs-31322/v1.
19. Krishnadev, P., Subramanian, K.S., Janavi, G.J., Ganapathy, S. and Lakshmanan, A., "Synthesis and Characterization of Nano-fibrillated Cellulose Derived from Green Agave americana L. Fiber." ***BioResources,*** Vol. 15, No. 2 (2020) 2442-2458. doi: 10.15376/biores.15.2.2442-2458
20. Zarina, Siti, and Ishak Ahmad. "Biodegradable composite films based on κ-carrageenan reinforced by cellulose nanocrystal from kenaf fibers." ***BioResources,*** Vol. 10, No. 1 (2015), 256-271. doi: 10.15376/biores.10.1.256-271
21. Kargarzadeh, Hanieh, Marcos Mariano, Jin Huang, Ning Lin, Ishak Ahmad, Alain Dufresne, and Sabu Thomas, "Recent developments on nanocellulose reinforced polymer nanocomposites: A review." ***Polymer,*** Vol. 132, (2017) 368-393. doi: 10.1016/j.polymer.2017.09.043
22. Teja Prathipati, S.R.R., Rao, C.B.K. and Dakshina Murthy, N.R., "Mechanical behavior of hybrid fiber reinforced high strength concrete with graded fibers." ***International Journal of Engineering, Transactions B: Applications,*** Vol. 33, No. 8 (2020), 1465-1471. doi: 10.5829/IJE.2020.33.08B.04
23. Chen, Wenshuai, Kentaro Abe, Kojiro Uetani, Haipeng Yu, Yixing Liu, and Hiroyuki Yano, "Individual cotton cellulose nanofibers: pretreatment and fibrillation technique." ***Cellulose,*** Vol. 21, No. 3, (2014), 1517-1528. doi: 10.1007/s10570-014-0172-z
24. Zhang, Wei, Zhennan Zhang, and Xinping Wang, "Investigation on surface molecular conformations and pervaporation performance of the poly(vinyl alcohol) (PVA) membrane." ***Journal of Colloid and Interface Science,*** Vol. 333, (2009), 346-353. doi: 10.1016/j.jcis.2009.01.058
25. Tang, Yufeng, Yumin Du, Yan Li, Xiaoying Wang, and Xianwen Hu, "A thermosensitive chitosan/poly (vinyl alcohol) hydrogel containing hydroxyapatite for protein delivery." ***Journal of Biomedical Materials Research Part A***: An Official Journal of The Society for Biomaterials, The Japanese Society for Biomaterials, and The Australian Society for Biomaterials and the Korean Society for Biomaterials, Vol. 91, (2009), 953-963. doi: 10.1002/jbm.a.32240
26. Ghaderi, Moein, Mohammad Mousavi, Hossein Yousefi, and Mohsen Labbafi, "All-cellulose nanocomposite film made from bagasse cellulose nanofibers for food packaging application." ***Carbohydrate Polymers,*** Vol. 104, (2014), 59-65. doi: 10.1016/j.carbpol.2014.01.013
27. Perumal, Anand Babu, Periyar Selvam Sellamuthu, Reshma B. Nambiar, and Emmanuel Rotimi Sadiku, "Development of polyvinyl alcohol/chitosan bio-nanocomposite films reinforced with cellulose nanocrystals isolated from rice straw." ***Applied Surface Science,*** Vol. 449, (2018), 591-602. doi: 10.1016/j.apsusc.2018.01.022
28. Huang, Yukun, Lei Mei, Xianggui Chen, and Qin Wang, "Recent developments in food packaging based on nanomaterials." ***Nanomaterials,*** Vol. 8, No. 10 (2018), 830. doi: 10.3390/nano8100830
29. Siró, István, and David Plackett, "Microfibrillated cellulose and new nanocomposite materials: a review." ***Cellulose,*** Vol. 17, No.3 (2010), 459-494. doi: 10.1007/s10570-010-9405-y
30. He, Wen, Shenxue Jiang, Qisheng Zhang, and Mingzhu Pan, "Isolation and characterization of cellulose nanofibers from Bambusa rigida." ***BioResources,*** Vol. 8, No. 4 (2013), 5678-5689. doi: 10.15376/biores.8.4.5678-5689
31. Yudhanto, F, Jamasri and Rochardjo, H.S.B., "Physical and Thermal Properties of Cellulose Nanofibers (CNF) Extracted from Agave Cantala Fibers Using Chemical-Ultrasonic Treatment." ***International Review of Mechanical Engineering,***

Vol. 12, No. 7, (2018), 597-603. doi: 10.15866/ireme.v12i7.14931

32. Yudhanto, F., Jamasri and Rochardjo, H.S.B., "Physical and Mechanical Characterization of Polyvinyl Alcohol Nanocomposite Made from Cellulose Nanofibers." In ***Materials Science Forum***, Trans Tech Publications Ltd. Vol. 988, (2020), 65-72. doi: 10.4028/www.scientific.net/MSF.988.65
33. Segal, L., Creely, J. J., Martin Jr., A.E., Conrad, C.M., "Anempirical method for estimating the degree of crystallinity ofnative cellulose using the X-ray diffractometer." ***Textile Research Journal,*** (1959), 786-794. doi: 10.1177/004051755902901003
34. Schick, C., "Differential scanning calorimetry (DSC) of semicrystalline polymers." ***Analytical and Bioanalytical Chemistry,*** Vol. 395, No. 6 (2009), 1589. doi: 10.1007/s00216-009-3169-y
35. Patel, Arunendra Kumar, R. Bajpai, and J. M. Keller, "On the crystallinity of PVA/palm leaf biocomposite using DSC and XRD techniques." ***Microsystem Technologies,*** Vol. 20, No.1 (2014), 41-49. doi: 10.1007/s00542-013-1882-0
36. Kong, Y., and J. N. Hay, "The measurement of the crystallinity of polymers by DSC." ***Polymer,*** Vol. 43, No.14 (2002), 3873-3878. doi: 10.1016/S0032-3861(02)00235-5
37. Rosa, M. F., Medeiros, E. S., Malmonge, J. A., Gregorski, K. S., Wood, D. F., Mattoso, L. H. C., ... & Imam, S. H, "Cellulose nanowhiskers from coconut husk fibers: Effect of preparation conditions on their thermal and morphological behavior." ***Carbohydrate Polymers,*** Vol. 81, No. 1 (2010), 83-92. doi: 10.1016/j.carbpol.2010.01.059
38. Shahbazi, P., Behzad, T., & Heidarian, P, "Isolation of cellulose nanofibers from poplar wood and wheat straw: optimization of bleaching step parameters in a chemo-mechanical process by experimental design", ***Wood Science and Technology,*** Vol. 51, No. 5, (2017), 1173-1187 doi: 10.1007/s00226-017-0929-2
39. Neto, W. P. F., Mariano, M., Da Silva, I. S. V., Silvério, H. A., Putaux, J. L., Otaguro, H., ... & Dufresne, "A. Mechanical properties of natural rubber nanocomposites reinforced with high aspect ratio cellulose nanocrystals isolated from soy hulls." ***Carbohydrate Polymers,*** Vol. 153, (2016), 143-152. doi: 10.1016/j.carbpol.2016.07.073
40. Hassan, M., Berglund, L., Hassan, E., Abou-Zeid, R., & Oksman, K., "Effect of xylanase pretreatment of rice straw unbleached soda and neutral sulfite pulps on isolation of nanofibers and their properties." ***Cellulose,*** Vol. 25, No.5 (2018), 2939-2953. doi: 10.1007/s10570-018-1779-2
41. de Morais Teixeira, E., Bondancia, T. J., Teodoro, K. B. R., Corrêa, A. C., Marconcini, J. M., & Mattoso, L. H. C., "Sugarcane bagasse whiskers: extraction and characterizations." ***Industrial Crops and Products,*** Vol. 33, No.1 (2011), 63-66. doi: 10.1016/j.indcrop.2010.08.009
42. Siqueira, G., Tapin-Lingua, S., Bras, J., da Silva Perez, D., & Dufresne, A, "Morphological investigation of nanoparticles obtained from combined mechanical shearing, and enzymatic and acid hydrolysis of sisal fibers." ***Cellulose,*** Vol. 17, No. 6 (2010), 1147-1158. doi: 10.1007/s10570-010-9449-z
43. Poletto, Matheus, Vinícios Pistor, and Ademir J. Zattera, "Structural characteristics and thermal properties of native cellulose." ***InTech,*** Vol. 10, (2013), 2705. doi: 10.5772/50452. 1
44. Khalil, HPS Abdul, H. Ismail, H. D. Rozman, and M. N. Ahmad, "The effect of acetylation on interfacial shear strength between plant fibres and various matrices." ***European Polymer Journal,*** Vol. 37, No. 5 (2001), 1037-1045. doi: 10.1016/S0014-3057(00)00199-3
45. Rezaei, S., Najafpour, G.D., Mohammadi, M. Moghadamnia, A.A. Kazemi., "Formic acid and microwave assisted extraction of curcumin from turmeric (*Curcuma longa* L.)." ***International Journal of Engineering. Transactions B: Applications,*** Vol. 29, No. 2 (2016), 145-151. doi: 10.5829/idosi.ije.2016.29.02b.02
46. Lim, Lim, Noor Rosli, Ishak Ahmad, Azwan Mat Lazim, and Mohd Mohd Amin, "Synthesis and swelling behavior of pH-sensitive semi-IPN superabsorbent hydrogels based on poly (acrylic acid) reinforced with cellulose nanocrystals." ***Nanomaterials,*** Vol. 7, No. 11 (2017), 399. doi: 10.3390/nano7110399
47. Sadeghifar, Hasan, and Arthur Ragauskas. "Lignin as a UV Light Blocker—A Review." ***Polymers,*** Vol. 12, No. 5 (2020): 1134. doi: 10.3390/polym12051134
48. Agrawal, lS L., and Arvind Awadhia, "DSC and conductivity studies on PVA based proton conducting gel electrolytes." ***Bulletin of Materials Science,*** Vol. 27, No. 6 (2004), 523-527. doi: 10.1007/BF02707280
49. Rynkowska, Edyta, Kateryna Fatyeyeva, Stéphane Marais, Joanna Kujawa, and Wojciech Kujawski, "Chemically and Thermally Crosslinked PVA-Based Membranes: Effect on Swelling and Transport Behavior." ***Polymers,*** Vol. 11, No.11, (2019), 1799. doi: 10.3390/polym11111799
50. Nishiyama, Yoshiharu, Paul Langan, and Henri Chanzy. "Crystal structure and hydrogen-bonding system in cellulose Iβ from synchrotron X-ray and neutron fiber diffraction." ***Journal of the American Chemical Society,*** Vol. 124, No. 31 (2002), 9074. doi: 10.1021/ja0257319

Persian Abstract

چکیده

در این مقاله یک مطالعه تجربی از افزودن نانوالیاف سلولزی (CNF) استخراج شده توسط فرآیند فراصوت شیمیایی از گیاهان برگ آگاو کانتالا در ماتریس پلی وینیل الکل (PVA)ارائه شده است. با ترکیب این مواد ، فیلم نانوکامپوزیتی با ضخامت 30 میکرومتر تولید می شود. ویژگی نانوکامپوزیت با افزودن CNF (0، 2 ، 5 ، 8 و 10 درصد وزنی) در تعلیق (3PVA درصد وزنی) بررسی شد. فیلم های نانوکامپوزیتی PVA / CNF با روش محلول ریخته گری تهیه شد. رشته های الیاف به CNF با استفاده از میکروسکوپ الکترونی روبشی و میکروسکوپ الکترونی عبوری مورد تجزیه و تحلیل قرار گرفت. پیوند شیمیایی مولکولی و تجزیه و تحلیل ساختاری گروه عملکردی فیلم نانوکامپوزیت با استفاده از پراش مادون قرمز و تبدیل اشعه ایکس تبدیل فوریه مورد آزمایش قرار گرفت. فیلم نانوکامپوزیت PVA / CNF دارای مزایای قابل توجهی در مانع ماورا بنفش ، پایداری حرارتی آزمایش شده توسط کالریمتری اسکن دیفرانسیل و تجزیه و تحلیل گرما و اندازه گیری مقاومت است. به طور کلی ، افزودن بهینه CNF در ماتریس 8 درصد وزنی است ، در نتیجه بالاترین شاخص تبلور (37/5 درصد) ، مقاومت کششی و کشیدگی در شکست به ترتیب 79 و 138 درصد افزایش داشت. دارای اشعه ماورا بنفش جذب کننده خوب (82/4 درصد) و پایداری حرارتی بالا (365 درجه سانتیگراد) است.